

Article

# Frequency-Octupling Millimeter-Wave Optical Vector Signal Generation via an I/Q Modulator-Based Sagnac Loop

Zhixian Yang <sup>1,\*</sup> , Kun Qu <sup>2</sup> and Xiang Liu <sup>3</sup><sup>1</sup> Institute of Information and Navigation, Air Force Engineering University, Xi'an 710000, China<sup>2</sup> China Xi'an Satellite Control Center, Xi'an 710000, China; m13259463680@163.com<sup>3</sup> College of Communications, National University of Defense Technology, Xi'an 710000, China; liuxiang\_0903@sina.com

\* Correspondence: yzx527@163.com

Received: 18 November 2018; Accepted: 8 January 2019; Published: 14 January 2019



**Abstract:** A new method for generating frequency-octupling millimeter-wave (mm-wave) vector signals in optical fields via a Sagnac loop is proposed. In this scheme, two orthogonally polarized fourth order sidebands can be obtained through an integrated dual-polarization quadrature phase shift keying (DP-QPSK) modulator. The two optical sidebands are sent into an I/Q modulator-based Sagnac loop. The I/Q modulator is modulated by a 16QAM baseband signal. In the Sagnac loop, one of the sidebands is modulated by the baseband vector signal along one direction, and the other sideband is unmodulated along the opposite direction because the I/Q modulator has the traveling-wave nature. Thanks to this modulation property and the symmetrical structure of the Sagnac loop, a frequency-octupling mm-wave vector signal that is free from interband beating and fiber chromatic dispersion interference can be generated by the photodetector (PD). After simulating a 20 km single-mode fiber (SMF) transmission, the generated frequency-octupling vector signal was good in function.

**Keywords:** frequency-octupling; vector signal generation; microwave photonics; Sagnac loop

## 1. Introduction

Greater requirements have been raised for the high-speed transmission of data, long-capacity services and the huge bandwidth of the communication system. Using a higher frequency to generate a mm-wave signal is perceived as a promising approach for future communication systems, due to its inherent wide bandwidth that can carry high-speed access data [1–4]. Traditionally, the mm-wave is generated from the low carrier frequency and restricted bandwidth of the electronic devices through electrical methods [5–9]. Because of intrinsic superiorities like anti-electromagnetic interference, low loss, large broadband and high frequency, mm-wave signal generation via photonic technology is being investigated to overcome these problems, which could play a crucial part in breaking the bottleneck of electronic bandwidth. Also, the mm-wave signal which is generated with vector modulation formats can remedy the limited frequency spectrum resources and data can be transmitted at a higher access rate. Thus, various methods for the generation of a vector signal are proposed using optical technology.

In recent years, scholars have investigated various precoding auxiliary schemes for the generation of photonic and mm-wave vector signals [10–12]. One scheme for the generation of a frequency octupling quadrature phase shift keying (QPSK) signal by precoding is proposed in Reference [10], another two schemes for the generation of frequency quadrupling QPSK signals and frequency

doubling 16QAM signals (also by precoding) are proposed in References [11,12], respectively. Different mm-wave vector signals with high frequencies can be generated through these schemes, thus decreasing the bandwidth demand of the devices. However, if two specific optical sidebands were removed by another expensive wavelength filter, this would reduce the signal-to-noise ratio (SNR). Scholars have also proposed some precoded schemes for the generation of mm-wave vector signals without using filters as an improvement [13,14]. A scheme that employed a single-drive MZM to generate a frequency-quadrupling QPSK signal was proposed in Reference [13]. The optical suppression ratio between the second and the fourth order sidebands is only 10 dB, which will decrease the SNR and not fit the high order QAM signal generation. High order vector signals, such as a QAM signal, can be generated by precoding without using a filter. However, this technique only can realize frequency-doubling [14]. The main issue perplexed in all these schemes is that the multiplication of amplitude or phase by frequency multiplication should instead be addressed through precoding. As a result, the transmitter will be complex in digital signal processing (DSP) [15,16]. A vector signal generation scheme without precoding and optical filter was proposed in Reference [15], which generated RF vector signals in the electrical domain and only realized frequency-doubling. Reference [16] proposed a scheme without precoding for the generation of a dual-tone QPSK signal which could select a QPSK modulated optical sideband and an unmodulated optical sideband. This scheme could finally can generate a frequency-nonupling QPSK signal, however, the correlative high order sidebands should be selected using an extra WSS (Wavelength Selective Switch).

In this work, an I/Q modulator-based Sagnac loop used to generate frequency-octupling 16QAM signals is proposed. Usually, the frequency-octupling signal can be generated by a DP-MZM, however the signal suffers from a low optical sideband suppression ratio (OSSR) because of the finite extinction ratio of the DP-MZM [17]. A DP-QPSK modulator is an integrated modulator that can flexibly generate different forms of optical signals and has been widely used in recent reports [18,19]. The proposed scheme consists of a DP-QPSK modulator, a tunable laser source (TLS) and an I/Q modulator-based Sagnac loop. The light wave is sent to the DP-QPSK modulator from the TLS. An optical carrier and  $\pm 4$ st-order optical sidebands can be generated in the DP-QPSK modulator by controlling the phases of the RF signal and adjusting the DP-QPSK modulator. Two orthogonally polarized  $\pm 4$ st-order optical sidebands with a suppressed optical carrier can be generated by a fiber Bragg grating (FBG), then the orthogonally polarized sidebands are split by a polarization beam splitter (PBS), which are sent to the Sagnac loop, where a 16QAM baseband signal is applied to the I/Q modulator. One of the 4st-order sidebands is modulated unidirectionally and the leaving sideband is unmodulated in the inverted direction because of velocity mismatch [20], thus the power fading effect can be eliminated. Finally, using a polarizer to combine and a photodetector (PD) to detect the two orthogonally polarized sidebands, a 16QAM vector signal with frequency-octupling can be generated. Employing the proposed scheme, our simulation demonstrated the generation of a 4 Gbaud 16QAM signal at 80 GHz by a 10 GHz RF signal, and the generated vector signal could achieve a 20 km SMF transmission with a BER of less than  $1 \times 10^{-3}$ . Comparing these results with the existing schemes, the scheme we proposed has key advantages in that it can meet the requirements for high frequency applications for frequency-octupling without precoding, and the signal is also immune to fiber chromatic dispersion since the baseband vector signal only modulates one sideband.

## 2. Principle

The frequency-octupling 16QAM vector signal generation scheme is proposed in Figure 1. In the scheme, a TLS sends a light wave to the DP-QPSK modulator, where three relatively pure sidebands can be generated, i.e., the optical carrier and the  $\pm 4$ st-order optical sidebands. The FBG is used to suppress the optical carrier. By adjusting the polarization controller (PC2), the optical signal is launched to the Sagnac loop from a PBS. The Sagnac loop contains an I/Q modulator and two polarization controllers (PCs). One sideband in the Sagnac loop transmitted clockwise while the other sideband transmitted counter-clockwise. A pulse patten generator (PPG) generated a 16QAM baseband signal which was

sent to the I/Q modulator. The I/Q modulator has a travelling-wave transmission property; for one sideband along the clockwise direction is almost unmodulated because of velocity mismatch, while the other counter-clockwise sideband can be sufficiently modulated by the baseband signal. Then, the orthogonally polarized  $\pm 4$ st-order sidebands are recombined in the PBS at the Sagnac loop output. The two sidebands are processed through a Pol and the square-law detection is operated through a PD to obtain a frequency-octupling 16QAM signal.

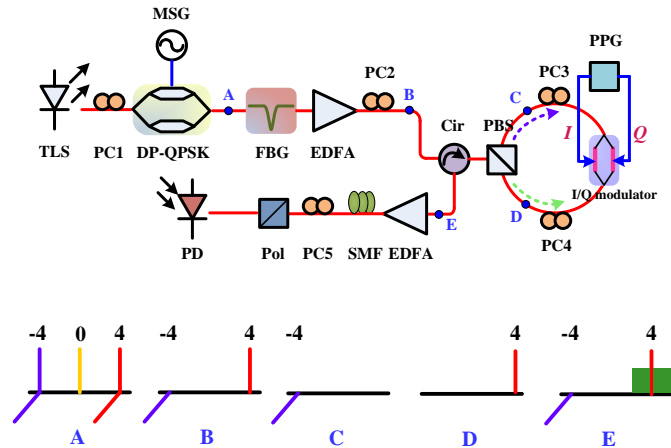


**Figure 1.** Schematic diagrams for the frequency-octupling 16QAM mm-wave signal generation and the spectra after different points.

The scheme generates  $\pm 4$ st-order optical sidebands through an integrated DP-QPSK modulator. We found that the spurious optical sidebands would emerge if we generated only a  $\pm 4$ st-order optical sideband. When  $\pm 4$ st-order optical sidebands and an optical carrier are generated simultaneously, no spurious optical sideband exists. The equivalent structure of the DP-QPSKM is shown in Figure 2. The RF signal is generated from a microwave signal generator (MSG) can be divided into four paths with different phases. The QPSK1 modulator and QPSK2 modulator can output optical signal, which is expressed as:

$$\begin{cases} E_1 = \cos(\omega_c t) [\cos(m \cos(\omega_{RF} t + \phi_1)) + \cos(m \cos(\omega_{RF} t + \phi_2))] \\ E_2 = \cos(\omega_c t) [\cos(m \cos(\omega_{RF} t + \phi_3)) + \cos(m \cos(\omega_{RF} t + \phi_4))] \end{cases} \quad (1)$$

where  $\omega_c$  and  $\omega_{RF}$  denote the angular frequency of the optical carrier and RF signal, respectively.  $\phi$  is the phase of RF signal and  $m = \frac{\pi v_m}{v_\pi}$  is the modulation index of the two QPSK modulators, where  $v_m$  and  $v_\pi$  are the driving voltage and half-wave voltage, respectively.

The deviations of the two QPSK modulators and the sub-MZMs are set as the maximum transmission point. Expanding Equation (1), the output signal can be written as:

$$\begin{cases} E_1 = e^{j\omega_c t} \left[ J_0(m) + 2 \sum_{n=1}^{\infty} (-1)^n J_{2n}(m) e^{j2n(\omega_{RF} t + \phi_1)} + J_0(m) + 2 \sum_{n=1}^{\infty} (-1)^n J_{2n}(m) e^{j2n(\omega_{RF} t + \phi_2)} \right] \\ E_2 = e^{j\omega_c t} \left[ J_0(m) + 2 \sum_{n=1}^{\infty} (-1)^n J_{2n}(m) e^{j2n(\omega_{RF} t + \phi_3)} + J_0(m) + 2 \sum_{n=1}^{\infty} (-1)^n J_{2n}(m) e^{j2n(\omega_{RF} t + \phi_4)} \right] \end{cases} \quad (2)$$

By adjusting the phases of the RF signal  $\phi_1 = 0, \phi_2 = \frac{\pi}{2}, \phi_3 = \frac{\pi}{8}, \phi_4 = \frac{5\pi}{8}$ , Equation (1) can be expressed as:

$$\begin{cases} E_1 = e^{j\omega_c t} \left[ 2J_0(m) + 4 \sum_{n=1}^{\infty} J_{4n}(m) e^{j4n\omega_{RF} t} \right] \\ E_2 = e^{j\omega_c t} \left[ 2J_0(m) + 4 \sum_{n=1}^{\infty} J_{4n}(m) e^{j4n(\omega_{RF} t + \frac{\pi}{2})} \right] \end{cases} \quad (3)$$

Equation (3) shows that there is an optical carrier and orthogonally polarized sidebands with orders of  $4_n$ . Spurious optical sidebands exist in the output signal. If modulation index  $m = 2.618$ ,  $J_0 \approx J_4$  and the spurious optical sidebands are ignorable. Thus, the  $\pm 4$ st-order optical sidebands and the optical carrier (three relatively pure sidebands) are generated. Following transmission through a wavelength fixed FBG, the optical carrier is well suppressed while pure  $\pm 4$ st-order optical sidebands are left untouched.

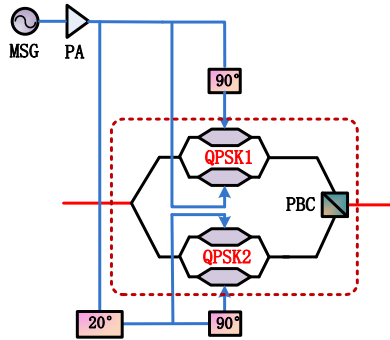


**Figure 2.** Configuration of the dual-polarization quadrature phase shift keying (DP-QPSK) modulator.

In the Sagnac loop, two binary data sequences drive the I/Q modulator. The 16QAM baseband signal can be generated through configuration. The baseband vector signal is as below:

$$E_b = [I(t) + jQ(t)]e^{j\omega_c t} \quad (4)$$

Then the Sagnac loop output is written as:

$$E_{out} = \begin{cases} J_4(m) \cos(\omega - 4\omega_{RF} + \frac{\pi}{2})t \\ \frac{1}{2} J_4(m) \{ \cos[(\omega_c + 4\omega_{RF})t + \beta E_b] + \cos[(\omega_c + 4\omega_{RF})t - \beta E_b] \} \end{cases} \quad (5)$$

where  $\beta$  represents the modulation index. The two orthogonally polarized signals are combined through a polarizer. The angle in the polarization direction is adjusted to  $\theta$  through PC5 (Polarization Controller5). The optical signal output from the polarizer is:

$$E_{Pol} = \cos \theta J_4(m) \cos(\omega_c - 4\omega_{RF} + \frac{\pi}{2})t + \frac{1}{2} \sin \theta J_4(m) \{ \cos[(\omega_c + 4\omega_{RF})t + \beta E_b] + \cos[(\omega_c + 4\omega_{RF})t - \beta E_b] \} \quad (6)$$

Equation (6) shows that the output signal is similar to an equivalent SSB modulation.  $L$  is the length of the SMF and  $\lambda$  is the propagation constant. The expression of the output signal after the SMF transmission is as below:

$$E_t = \cos \theta J_4(m) \cos(\omega_c - 4\omega_{RF} + \frac{\pi}{2})t + \frac{1}{2} \sin \theta J_4(m) \left\{ \cos[(\omega_c + 4\omega_{RF})t + \beta [I(t - \frac{\lambda L}{\omega_c}) + jQ(t - \frac{\lambda L}{\omega_c})] e^{j(\omega_c t - \lambda L)}] + \cos[(\omega_c + 4\omega_{RF})t - \beta [I(t - \frac{\lambda L}{\omega_c}) + jQ(t - \frac{\lambda L}{\omega_c})] e^{j(\omega_c t - \lambda L)}] \right\} \quad (7)$$

After detection through the square-law PD, the output electrical signal can be written as:

$$I_t \propto \frac{1}{4} \cos \theta \sin \theta J_4^2(m) \left\{ 2I(t - \frac{\lambda L}{\omega_c}) \cos[\lambda L(\omega_c - 8\omega_{RF} + \frac{\pi}{2})t] + 2Q(t - \frac{\lambda L}{\omega_c}) \sin[\lambda L(\omega_c - 8\omega_{RF} + \frac{\pi}{2})t] \right\} \quad (8)$$

Equation (8) shows that a vector signal with a frequency of  $8\omega_{RF}$  can be obtained and that the system is free from power fading caused by fiber dispersion.

### 3. Simulation Results

The proposed frequency-occluding vector signal scheme was simulated by OptiSystem 7.0. In Figure 1, the light wave from the TLS was 10 dBm with a 1 MHz line width, working at 193.1 THz. The light wave was injected into the DP-QPSK modulator through PC1. The DP-QPSK modulator was driven by the RF signal generated by MSG. Its frequency was 10 GHz and modulation index was 2.618. Figure 2 shows the optical signal with  $\pm 4$ st-order sidebands and the optical carrier which could be obtained by changing the phases of the RF signal. The optical spectra from the DP-QPSK modulator is shown in Figure 3a. The FBG is centered at 193.1 THz to suppress the optical carrier, Figure 3b illustrates the optical sidebands with a frequency spacing of 80 GHz. After being amplified by an EDFA (Erbium Doped Fiber Amplifier), the generated signal is launched into the Sagnac loop.

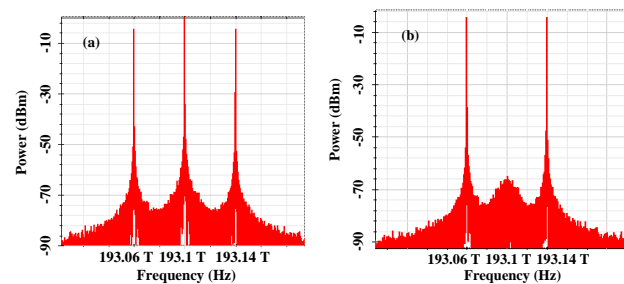


**Figure 3.** The output optical spectra of the (a) DP-QPSK modulator and (b) fiber Bragg grating (FBG).

In the Sagnac loop, 4 Gbaud baseband binary signals generated from a PPG, which has a pseudo-random binary sequence (PRBS) of  $2^{13} - 1$ , are applied to I/Q modulator. Figure 4a shows the electrical spectra and Figure 4b shows the constellation of the baseband signal. A PBS is used to combine the two sidebands from the Sagnac loop. The optical spectra at the output of the PBS is shown in Figure 5a. It is shown that one of the optical sidebands that transmitted counter-clockwise was modulated through the baseband signal, while the other optical sideband that transmitted clockwise was unmodulated due to the travelling-wave transmission property of the I/Q modulator. After transmission over 20 km of SMF, when the PMD (Polarisation Mode Dispersion) coefficient was  $0.5 \text{ ps/km}^{1/2}$ , the dispersion slope was  $0.075 \text{ ps/nm}^2 \cdot \text{km}$ , the attenuation coefficient was  $0.2 \text{ dB/km}$  and the chromatic dispersion was  $16.75 \text{ ps/nm} \cdot \text{km}$ . The orthogonally polarized sidebands were sent to the polarizer and then received by the PD. Figure 5b shows the RF spectra of the generated vector mm-wave signal. A 16QAM mm-signal at 80 GHz was generated when the modulated sideband and the unmodulated sideband beat each other.

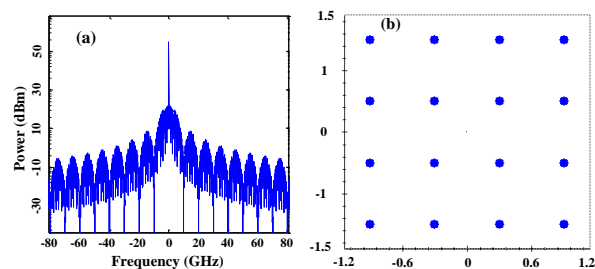


**Figure 4.** (a) The electrical spectra and (b) the constellation of the baseband signal.

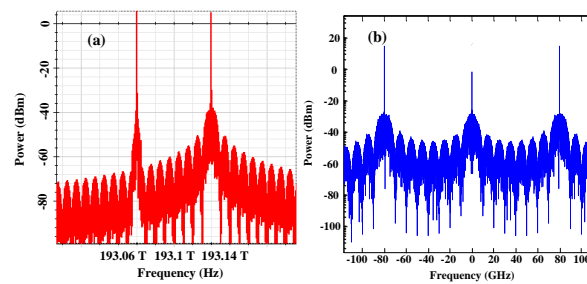


**Figure 5.** (a) The output optical spectra of the polarization beam splitter (PBS). (b) The output electrical spectra of the photodetector (PD).

The 16QAM signal was demodulated by an 80 GHz signal after being transmitted 20 km in SMF. The eye diagrams of the I and Q branches are shown in Figure 6a,b, indicating that the eyes were opening. The received vector signal constellation is clear and symmetrical in Figure 6c.

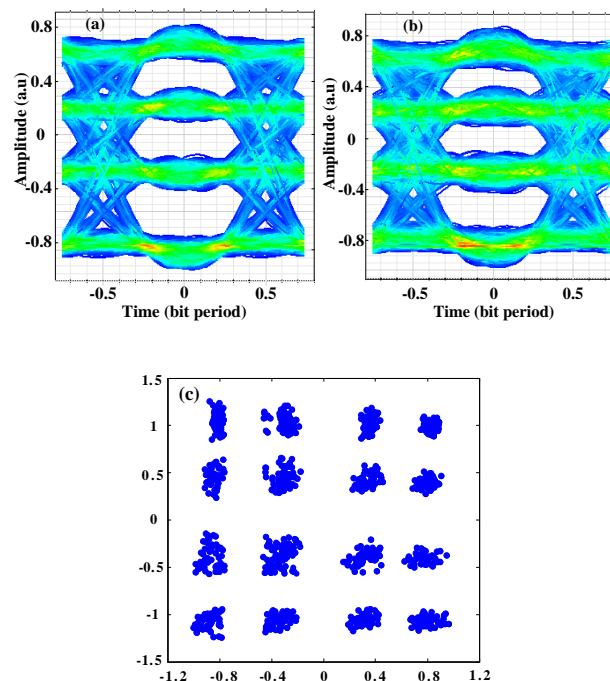


**Figure 6.** Eye diagrams of the (a) I branch and the (b) Q branch of the 16QAM signal at 80 GHz after a 20 km single-mode fiber (SMF) transmission. (c) The generated 16QAM signal constellation at 80 GHz after a 20 km SMF transmission.

The BER of the 80 GHz vector signal with varying input power for different transmission cases was simulated. Figure 7a shows the BER curves of the 16QAM signal at 80 GHz (2 and 4 Gbaud) after a 20 km SMF transmission. The BER was under  $1 \times 10^{-3}$  when the power of the received optical signal was larger than  $-5.8$  dBm or  $-4$  dBm. The 4 Gbaud 16QAM signal caused a 1.8 dB power penalty versus the 2 Gbaud case. Figure 7b shows the measured BER curves of the 16QAM signal with 4 Gbaud at 80 GHz in the condition of BTB and a 20 km SMF transmission. When the received optical power was greater than  $-5.5$  dBm and  $-4$  dBm, the BER was under  $1 \times 10^{-3}$ . Therefore, a 1.5 dB power penalty was caused. In the system, the main imperfection that could introduce noise is the insertion loss of the MZM, it is 5–7 dB. However, only one of the  $\pm 4$ st-order sidebands is modulated, meaning that power fading due to the fiber dispersion in generated signal is well suppressed. Thanks to this modulation form, the influence of beat noise on the system can be better reduced. The scheme we proposed is free from fiber chromatic dispersion. It can be seen the results agree with our theoretical analysis well.

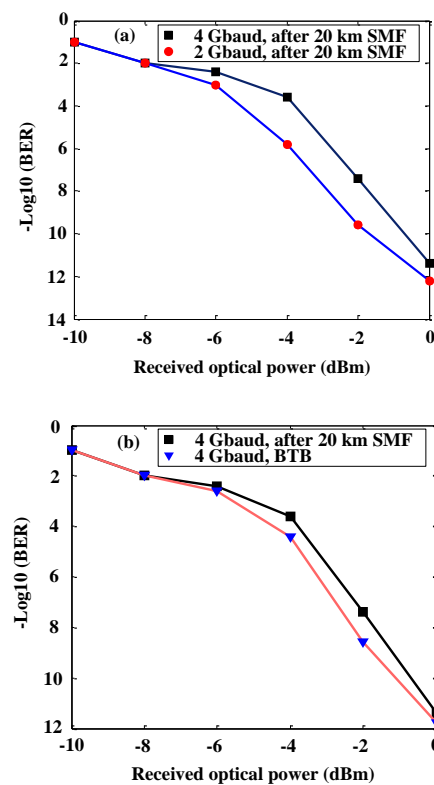


**Figure 7.** BER versus received optical power in the case of a (a) 2 and 4 Gbaud 16QAM signal after a 20 km SMF transmission. (b) BTB and a 20 km SMF transmission.

#### 4. Conclusions

A new photonic generation scheme for a 16QAM frequency-doubling signal without precoding was proposed. A DP-QPSK modulator and an FBG were configured to generate orthogonally polarized  $\pm 4$ st-order sidebands. After being combined by a PBS, the two optical sidebands were sent into an I/Q modulator-based Sagnac loop. One of the sidebands was modulated by the baseband signal and the other was unmodulated. The proposed scheme is not affected by environmental disturbances and power fading. Moreover, the eye diagrams, the BER curves and the constellations of the frequency-octupling 16QAM signal were analyzed to verify the performance of the proposed scheme.

**Author Contributions:** All authors read and approved the final manuscript.

**Funding:** This research received no external funding.

**Acknowledgments:** We would like to acknowledge Xidian University for supporting the experimental platform.

**Conflicts of Interest:** The authors declare no conflict of interest.

#### References

1. Kitayama, K.; Maruta, A.; Yoshida, Y. Digital coherent technology for optical fiber and radio-over-fiber transmission systems. *J. Lightw. Technol.* **2014**, *32*, 3411–3420. [[CrossRef](#)]
2. Huang, H.T.; Liang, W.L.; Lin, C.T.; Wei, C.C.; Chi, S. 100-GHz DD-OFDM-RoF system over 150-km fiber transmission employing pilot-aided phase noise suppression and bit-loading algorithm. *Opt. Exp.* **2014**, *22*, 3938–3943. [[CrossRef](#)] [[PubMed](#)]
3. Li, X.; Dong, Z.; Yu, J.; Chi, N.; Shao, Y.; Chang, G.K. Fiber-wireless transmission system of 108 Gb/s data over 80 km fiber and  $2 \times 2$  multiple-input multiple-output wireless links at 100 GHz W-band frequency. *Opt. Lett.* **2012**, *37*, 5106–5108. [[CrossRef](#)] [[PubMed](#)]
4. Wells, J. Faster than fiber: The future of multi-Gb/s wireless. *IEEE Microw. Mag.* **2009**, *10*, 104–112. [[CrossRef](#)]

5. Yu, J.; Jia, Z.; Yi, L.; Su, Y.; Chang, G.-K.; Wang, T. Optical millimeter-wave generation or up-conversion using external modulators. *IEEE Photon. Technol. Lett.* **2006**, *18*, 265–267.
6. Lin, C.-T.; Shih, P.-T.; Jiang, W.-J.; Wong, E.-Z.; Chen, J.J.; Chi, S. Photonic vector signal generation at microwave/millimeter-wave bands employing an optical frequency quadrupling scheme. *Opt. Lett.* **2010**, *34*, 2171–2173. [[CrossRef](#)] [[PubMed](#)]
7. Li, W.; Yao, J. Microwave generation based on optical domain microwave frequency octupling. *IEEE Photon. Technol. Lett.* **2010**, *22*, 24–26. [[CrossRef](#)]
8. Zhang, J.; Chen, H.; Chen, M.; Wang, T.; Xie, S. A photonic microwave frequency quadrupler using two cascaded intensity modulators with repetitious optical carrier suppression. *IEEE Photon. Technol. Lett.* **2007**, *19*, 1057–1059. [[CrossRef](#)]
9. Yu, J.; Jia, Z.; Wang, T.; Chang, G.K. Centralized lightwave radio-over-fiber system with photonic frequency quadrupling for high-frequency millimeter-wave generation. *IEEE Photon. Technol. Lett.* **2007**, *19*, 1499–1501. [[CrossRef](#)]
10. Li, X.; Yu, J.; Xiao, J.; Chi, N.; Xu, Y. W-band PDM-QPSK vector signal generation by MZM-based photonic frequency octupling and precoding. *IEEE Photon. J.* **2015**, *7*, 7101906. [[CrossRef](#)]
11. Li, X.; Zhang, J.; Xiao, J.; Zhang, Z.; Xu, Y.; Yu, J. W-band 8QAM vector signal generation by MZM-based photonic frequency octupling. *IEEE Photon. Technol. Lett.* **2015**, *27*, 1257–1260. [[CrossRef](#)]
12. Zhao, L.; Yu, J.; Chen, L.; Min, P.; Li, J.; Wang, R. 16QAM vector millimeter-wave signal generation based on phase modulator with photonic frequency doubling and precoding. *IEEE Photon. J.* **2016**, *8*, 5500708. [[CrossRef](#)]
13. Li, X.; Yu, J.; Chang, G. Frequency-quadrupling vector mm-wave signal generation by only one single-drive MZM. *IEEE Photon. Technol. Lett.* **2016**, *28*, 1302–1305. [[CrossRef](#)]
14. Dong, Z. 64QAM vector radio-frequency signal generation based on phase precoding and optical carrier suppression modulation. *IEEE Photon. J.* **2016**, *8*, 2630306. [[CrossRef](#)]
15. Wang, Y.; Yu, J.; Li, X.; Xu, Y.; Chi, N.; Chang, G.K. Photonic vector signal generation employing a single-drive MZM-based optical carrier suppression without precoding. *J. Lightw. Technol.* **2015**, *33*, 5235–5241. [[CrossRef](#)]
16. Ma, J. Dual-tone QPSK optical millimeter-wave signal generation by frequency nonupling the RF signal without phase precoding. *IEEE Photon. J.* **2016**, *8*, 2630306. [[CrossRef](#)]
17. Li, X.; Zhao, S.; Zhang, Y.; Zhu, Z.; Pan, S. Generation of a frequency-quadrupled phase-coded signal with large tunability. *IEEE Photon. Technol. Lett.* **2016**, *28*, 1980–1983. [[CrossRef](#)]
18. Gao, Y.; Wen, A. Analog Photonic Link with Tunable Optical Carrier to Sideband Ratio and Balanced Detection. *IEEE Photon. J.* **2017**, *9*, 7200510. [[CrossRef](#)]
19. Zhang, Y.; Zhang, F.; Pan, S. Generation of Frequency-Multiplied and Phase-Coded Signal Using an Optical Polarization Division Multiplexing Modulator. *IEEE Trans. Microw. Theory Technol.* **2017**, *65*, 651–660. [[CrossRef](#)]
20. Li, W.; Yao, J. Dynamic range improvement of a microwave Photonic link based on bi-directional use of a polarization modulator in a Sagnac loop. *Opt. Exp.* **2013**, *21*, 15692–15697. [[CrossRef](#)] [[PubMed](#)]

